Water Microdroplets on Molecularly Tailored Surfaces: Correlation between Wetting Hysteresis and Evaporation Mode Switching

Dinah M. Soolaman and Hua-Zhong Yu*

Department of Chemistry, Simon Fraser University, Burnaby, British Columbia V5A 1S6, Canada

Received: March 7, 2005; In Final Form: July 31, 2005

The evaporation of water microdroplets from solid surfaces was studied using digital contact angle analysis techniques. An inclusive trend for the evaporation process, that is, a switch from the initial constant contact *area* to the subsequent constant contact *angle* mode was observed for all surfaces examined, including mixed self-assembled monolayers (SAMs) on gold and "conventional" surfaces such as silicon wafers, polycarbonate, and Teflon. More importantly, it has been shown that the change in contact angle during the evaporation process (i.e., evaporation hysteresis, $\Delta\theta_{evap}$, the difference between the initial and "equilibrated" contact angle) correlates well with the wetting hysteresis determined directly (i.e., measuring the advancing and receding contact angles on these surfaces by changing the drop volume). The comparison between mixed SAM surfaces and conventional solids revealed that the evaporation/wetting hysteresis is dominated by the roughness (from nanometer to micrometer scale) rather than the chemical heterogeneity of the surface. The evaporation rates of water microdroplets on these surfaces were also monitored and modeled.

1. Introduction

Evaporation of water microdroplets is a fundamental phenomenon in nature that is vital to many life processes. As noted by Rusdi and Moroi in their recent publication,[1] the beginning of the 20th century marked the first recorded study of the evaporation process of water on a surface covered with an insoluble monolayer.[2] Since then, there have been numerous studies that focus primarily on the evaporation rate of liquids from solid surfaces, which is traditionally measured as the change in mass of the liquid per unit time.[3−7] Picknett and Bexon in 1977 extended the investigation beyond evaporation rates, which led to the classification of the overall process into two distinct modes (i.e., the variation of the droplet shape as a function of time).[6] As depicted in Scheme 1, the first is the constant contact *area* mode, for which the contact area remains unchanged during evaporation while the contact angle decreases ("pinning"). The second is known as the constant contact *angle* mode where the contact angle remains unchanged during evaporation but the contact area decreases ("shrinking"). They proposed that during evaporation the first mode dominates until the contact angle decreases to a constant value, and at this point the evaporation switches to the second mode; however, this was not shown experimentally. Later, Birdi and Vu studied the evaporation of water droplets on two "smooth" surfaces: glass and Teflon.[7] Their results led to two generalizations: (i) if the contact angle $\theta < 90°$, the constant contact area mode is observed, and (ii) if $\theta > 90°$, the constant contact angle mode would be expected.[7a] It should be noted that the variation of the morphology and chemical composition of these surfaces were not considered. Two years later, Shanahan and co-workers studied the evaporation of water on various substrates (i.e., poly(tetrafluoroethylene), polyethylene, glass, and epoxy resin) with a range of roughness under different atmospheric conditions.[8] They monitored the height, diameter, and contact angle of water droplets during evaporation in both open and closed systems and observed complex patterns for these systems. The evaporation process was divided into four stages, with each stage showing different changes in the water droplet shape. For example, when the atmosphere is not saturated, there is a pronounced decrease in height and contact angle while the drop diameter remains constant. This is, essentially, the first mode (constant contact area) observed by Picknett and Bexon.[6]

SCHEME 1

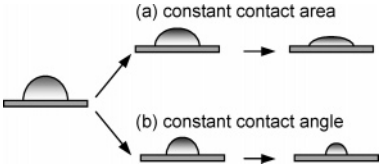

All these pioneering studies suggest that understanding the water evaporation phenomenon requires knowledge of the wetting properties of the surface, particularly the wetting hysteresis. It is defined as the difference between advancing and receding contact angles,[9] that is, the tendency of liquid droplets to advance and recede, respectively, across a surface which is related to the movement of a three-phase (solid−liquid−vapor) contact line.[10] The wetting hysteresis is a result of the adhesion created between the liquid and solid during spreading/receding.[9] Since the work of Young in the early 19th century on the contact angles of liquids on smooth solid surfaces, a significant amount of research has been devoted to understanding this common dynamic process by studying how surface defects and chemical heterogeneity affect both the adhesive nature and contact angle hysteresis of water droplets.[10] The ability to manipulate these two factors would allow for the potential control of surface wetting properties that are critical to numerous industrial and biological applications such as waterproofing, insecticide spraying, evaporation processes occurring in engines, and protein adsorption.[7,10] Since the observation that there exists a range of contact angles on surfaces rather

* Author to whom correspondence should be addressed. E-mail: hzyu@sfu.ca.

10.1021/jp051182s CCC: $30.25 © 2005 American Chemical Society
Published on Web 08/31/2005

than the single value predicted by Young's theory, numerous experiments have been done to understand this apparent deviation.[11] Although this phenomenon has been analyzed from a thermodynamic perspective, considering the energy barriers between the metastable contact angles, wetting hysteresis is still not well understood. Recently, Extrand studied the wetting properties of polyamide and polyethylene surfaces and suggested that roughness does not strongly influence wetting hysteresis, but rather it is dominated by the molecular interactions between the liquid and the solid surface.[9]

The advancement of self-assembly techniques has provided an opportunity to study the effects of chemical heterogeneity and molecular level roughness on wetting properties.[12] We[13] and others[14−16] have demonstrated that, in mixed self-assembled monolayers (SAMs) containing polar and nonpolar components of similar chain length, the wetting hysteresis is not correlated to the polarity or chemical composition of the surface. Although the experimental conditions differed in regard to the relative humidity and incubation time, the general findings suggested that chemical heterogeneity does not dominate contact angle hysteresis.[13−16] Contrasting results were obtained by Semal et al. who found that the wetting hysteresis was maximal on mixed SAMs that were 50% hydroxylated.[17] Folkers et al. studied the influence of chain length of mixed SAMs and discovered that large contact angle hysteresis exists when significant disorder occurs between the monolayer and the contacting liquid.[18] Additionally, in mixed short/long-chain SAMs, a larger hysteresis was found when the longer chain was terminated with a polar group (−OH) and the shorter chain with a nonpolar group ($-CH_3$). These studies indicated that the contact angle hysteresis is influenced by the surface roughness at the molecular level.

We have recently demonstrated that organic monolayers can be used as model systems to understand the evaporation phenomenon; our preliminary experiments showed the presence of two distinct evaporation modes for water droplets on mixed SAMs on gold.[13] On these mixed alkanethiolate SAMs of approximately the same chain length, the effects of surface roughness are minimized.[17,19] By varying the ratio of polar (−OH) and nonpolar ($-CH_3$) groups in the SAMs, the surface energy (hydrophobicity/hydrophilicity) can be easily tuned. We have found that the evaporation mode switching is independent of surface hydrophobicity but correlates with the wetting hysteresis in the previous study.[13] The present study extends these investigations to mixed monolayers (i.e., −OH- and $-CH_3$-terminated) of different chain lengths on gold surfaces to investigate the effect of roughness at the molecular level. For generalization, other conventional solid materials, specifically Teflon, silicon wafers, and polycarbonate, were also examined.

2. Experimental Section

Gold substrates (regular glass slides first covered with 10-nm Cr, followed by 100-nm Au) were purchased from Evaporated Metal Films (EMF) Inc. (Ithaca, NY); 11-mercapto-1-undecanol (97%), 1-octanethiol (98.5+%), 1-decanethiol (96%), and 1-octadecanethiol (98%) from Aldrich; silicon (111) wafers (n-type) from Virginia Semiconductor, Inc. (Fredericksburg, VA); poly(tetrafluoroethylene) (Teflon) sheets from the local machine shop; and polycarbonate bases of CDs from Millennium Compact Disk Industries, Inc. (Vancouver, BC). Deionized water (>18.3 Ω cm) was produced from a Barnstead EasyPure UV/UF compact water system (Dubuque, IA).

The silicon wafers and Teflon were cleaned by immersion in "piranha" solution (3:1 mixture of concentrated H_2SO_4 and H_2O_2 (30%)) for 30 min at 90 °C (CAUTION: use extreme care as piranha is explosive when in contact with organic materials), and then rinsed with deionized water. Gold slides were also cleaned in piranha solution but for a shorter period (5 min at 90 °C), followed by copious rinsing with water; they were then incubated in deposition solutions containing two thiols (11-mercapto-1-undecanol/1-octanethiol, 11-mercapto-1-undecanol/1-octadecanethiol, or 11-mercapto-1-undecanol/1-decanethiol) in 95% ethanol (total concentration 1.0 mM) for approximately 24 h at ambient conditions. It has been found by Bain et al. that there was no significant effect on the quality of the monolayers when the incubation time varies from overnight to two months.[14] After removal from the deposition solution, the substrates were washed with ethanol and water sequentially and dried under nitrogen. Polycarbonate substrates were sonicated in ethanol for 10 min and rinsed with water.

A digital AST Optima contact angle apparatus with a horizontal light beam to illuminate the liquid droplet was used to monitor the evaporation process and measure the contact angles. Water microdroplets (1−5 μL with an uncertainty of less than 10%) were delivered to the substrates from automatic micropipets. Analysis of the evaporation process under ambient conditions (temperature: 20 ± 3 °C, humidity: $30 \pm 5\%$) was performed with software provided by the manufacturer. Droplets were monitored until they had completely evaporated. In practice, enlarged digital pictures of the droplet taken at 1-min intervals were fitted to spherical-cap geometry in order to calculate the contact area, contact angle, and drop volume. In the range 30−120° the precision was ±0.5°, better than what is achievable with a contact angle goniometer. However, the reproducibility of the measurements over different areas of the same sample (with different droplets) was only ±2°. The advancing and receding contact angles were measured by the method of Dettre and Johnson.[20]

Atomic force microcopy (AFM) images were obtained from a custom-made instrument with a silicon nitride tip (Triangular D of MSCT-AUHW, Veeco Metrology group, resonance frequency 15 kHz, force constant 0.03 N/m). Areas of two different sizes (1 μm × 1 μm and 2 μm × 2 μm) were scanned in contact mode. AFM images were analyzed by calculating the root-mean-square (RMS) roughness factor:[21]

$$f_{\mathrm{RMS}} = \sqrt{\frac{1}{n}\sum_{i=1}^{n}(z_i - \bar{z})^2}$$

3. Results

An understanding of how water microdroplets interact with solid surfaces and how the shape varies with time is essential for tuning the surface to have certain desired wetting properties. In our studies, the evaporation of water microdroplets from various substrates was followed by monitoring the contact angle, contact area, and drop volume as a function of time with the help of a digital contact angle apparatus. Mixed monolayers consisting of polar (−OH) and nonpolar ($-CH_3$) terminal groups of different chain lengths on gold were compared to determine if the evaporation modes are affected by the roughness at the molecular level. Other conventional surfaces, such as Teflon, silicon wafer (a model system for semiconductor materials), and polycarbonate (a widely used polymeric substrate) that have totally different wetting properties and surface morphologies were also tested. The wetting hysteresis was measured subsequently on all surfaces and compared to the contact angle change during evaporation. In all cases, AFM images were obtained to

SCHEME 2

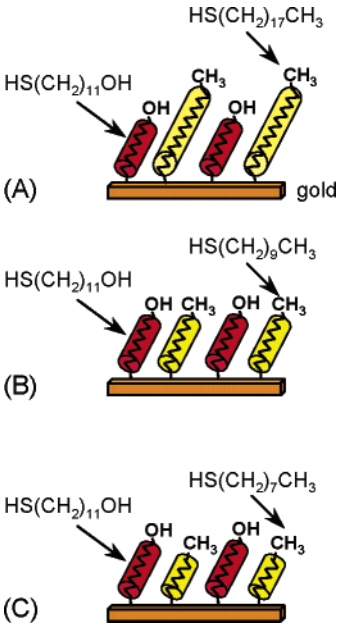

provide a better understanding of the correlation between the surface morphology and the evaporation process.

3.1. Mixed SAMs Prepared from Thiols of Different Chain Lengths. Three binary SAMs consisting of the following alkanethiols in 1:1 molar ratios (in the deposition solution) were examined (Scheme 2): (A) 1-octadecanethiol/11-mercapto-1-undecanol (C18/C11OH), (B) 1-decanethiol/11-mercapto-1-undecanol (C10/C11OH), and (C) 1-octanethiol/11-mercapto-1-undecanol (C8/C11OH).[22] By maintaining the same substrate (gold films deposited on glass slides under vacuum), the underlying surface morphology is kept unchanged, and any variation in roughness is mainly a consequence of the different molecular lengths in the mixed monolayer. In Figure 1, we have shown the evaporation behavior of water microdroplets on these model surfaces by monitoring the contact angle (A) and contact area (B), respectively, as a function of time. Although the molar ratio between polar and nonpolar groups remained the same for the three binary SAMs, their initial contact angles are different, presumably because of the different *n*-alkanethiol chain lengths. The C18/C11OH SAM is more hydrophobic than C10/C11OH, which in turn is more hydrophobic than C8/C11OH, since exposure of the longer chain termini to the wetting environment masks the effect of the functional group on the shorter chain.[23] In all cases, when a water microdroplet was placed on the SAM surface, initially the contact angle decreased while the contact area remained constant. For C18/C11OH and C10/C11OH SAMs after approximately 5 min, the contact area began decreasing as the contact lines began to move inward (shrinking) while the contact angle remained constant. A similar trend was observed for C8/C11OH; however, the switch to constant contact angle mode occurred after a longer period of about 10 min. No dependence has been observed on the water droplet volumes when they were kept relatively small (1−5 μL); however, the behavior of larger droplets (>5 μL) is no longer dominated by surface tension effects as gravity begins to play a significant role.

The evaporation hysteresis ($\Delta\theta_{evap}$) is defined as the difference between the initial (θ_i) and the "equilibrated" contact angle (θ_c) (the constant angle reached after the initial decrease) that is extrapolated from the plot in Figure 1A. Although the three mixed SAMs show the same trend, they displayed distinct

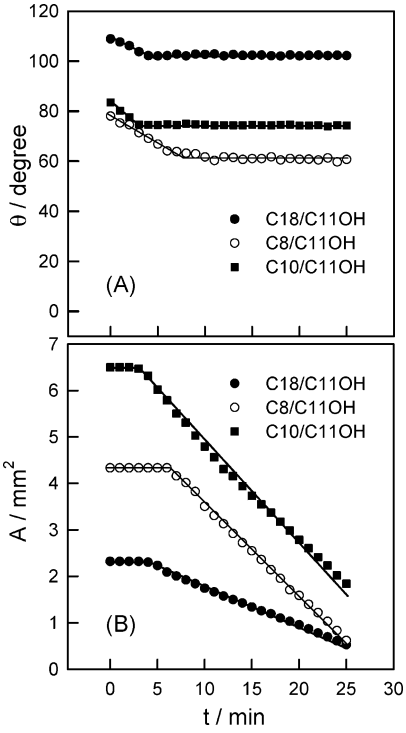

Figure 1. Evaporation of water microdroplets from mixed SAMs on gold under ambient conditions. (A) Contact angle as a function of time. (B) Contact area as a function of time. Each mixed SAM consists of a 1:1 molar ratio of the two specified alkanethiols (in the deposition solution).

TABLE 1: Correlation between Surface Roughness, Evaporation Hysteresis, and Directly Measured Wetting Hysteresis

surface	RMS roughness factor (Å)[a]	RMS roughness factor (Å)[b]	evaporation hysteresis (°)	wetting hysteresis (°)[c]
C8/C11OH/Au	31.4	56.6	16.9 ± 2.0	16.6 ± 1.5
C10/C11OH/Au			9.5 ± 0.5	10.0 ± 0.4
C18/C11OH/Au	26.8	46.1	6.5 ± 2.8	7.0 ± 0.7
Teflon	138.2		19.4 ± 3.0	20.9 ± 3.2
silicon oxide	24.6	46.4	10.0 ± 1.5	10.7 ± 2.8
polycarbonate		68.4	8.9 ± 2.0	10.0 ± 1.0

[a] The root-mean-square (RMS) roughness factor (AFM studies) is calculated for a 1 μm × 1 μm area. [b] RMS roughness factor for a 2 μm × 2 μm area. [c] Directly measured difference between advancing and receding contact angles.

differences in the evaporation hysteresis, and that are apparently sensitive to variations of the *n*-alkanethiol chain lengths. As shown in Table 1, $\Delta\theta_{evap}$ for C8/C11OH is considerably larger than that for C10/C11OH and C18/C11OH.

Direct measurements of wetting hysteresis ($\Delta\theta$), the difference between advancing (θ_A) and receding (θ_R) contact angles, using the method of Dettre and Johnson, were conducted on these surfaces for comparison. The results ($\Delta\theta = \theta_A - \theta_R$) agreed very well in magnitude with $\Delta\theta_{evap}$ (Table 1) for the three mixed SAMs. This finding is of significance because it confirms our hypothesis that the evaporation mode switching is dominated by the wetting hysteresis of the surface, as indicated previously on the mixed SAMs bearing molecules of the same alkyl chain lengths.[13] It also demonstrates that one can accurately determine the wetting hysteresis from the evaporation trend of a liquid from a solid surface. The C18/C11OH surface was thought to be molecularly rougher due to the long C18 chains; therefore, a larger contact angle hysteresis would have been expected.[24,25] In reality, a smaller evaporation

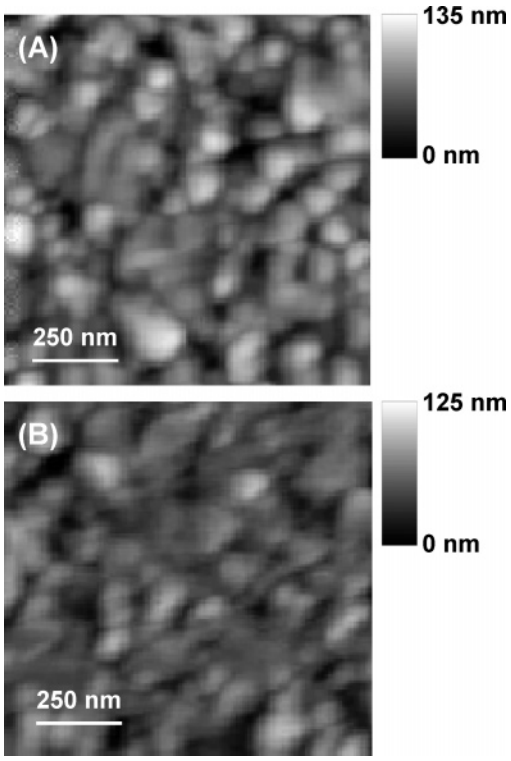

Figure 2. Contact mode AFM images of (A) C18/C11OH and (B) C8/C11OH SAMs on gold.

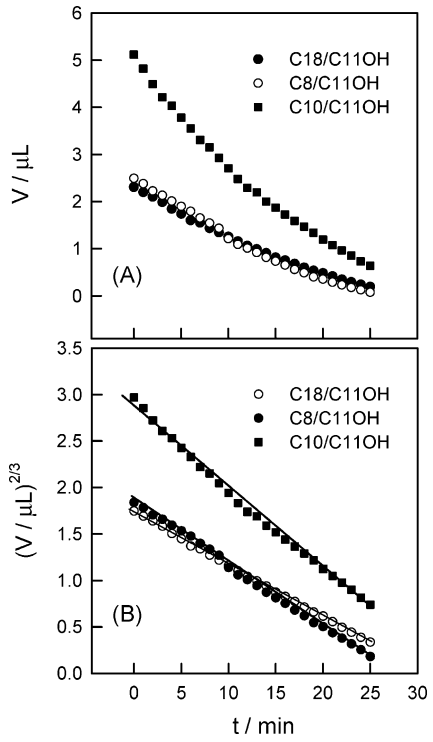

Figure 3. Evaporation rate of water microdroplets from mixed SAM surfaces. (A) Drop volume (V) as function of evaporation time (t). (B) Linear relationship between $V^{2/3}$ and t.

hysteresis for C18C11OH surface was observed compared with the C8/C11OH system (Table 1). Folkers et al. have shown that for mixed short/long chain systems a larger wetting hysteresis is observed when the longer chain is terminated with a polar group (−OH).[18] Our results may also be explained by the denser packing of mixed SAMs with long CH_3-terminated and short OH-terminated chains. Atre et al. have demonstrated that, in these mixed SAMs, adjacent long CH_3-terminated chains are organized in clusters and bend away from the shorter underlying OH-terminated chains,[23] which may decrease the surface roughness at the molecular level. As a result, the surface roughness for mixed SAMs on gold is primarily determined by the topography of the underlying gold substrates, as verified subsequently by AFM studies. While the rolling hill topography expected for gold substrates (prepared by vacuum evaporation) was observed, there is no significant difference between the two mixed monolayers (Figure 2). The RMS roughness factors were calculated for both a 2 μm × 2 μm and a 1 μm × 1 μm area (Table 1). The C18/C11OH system was indeed slightly smoother and had a smaller RMS roughness factor than the C8/C11OH system. This result correlates well with both the evaporation hysteresis and directly measured wetting hysteresis, suggesting that a rougher surface would have a larger wetting hysteresis.

Analyzing the evaporation rates of these systems, the volumes of the water microdroplets were found to decrease nonlinearly with time (Figure 3A); this indicates that the evaporation rates change as a function of time. According to the empirical model proposed by Rowan and Erbil based on the spherical drop assumption, $V^{2/3}$ versus t plots are expected to be linear.[4,26] In Figure 3B, we have shown that the evaporation of water from all three mixed SAMs does indeed follow this model. In addition, it can be concluded that the more hydrophilic a surface, the faster is the evaporation rate, which is consistent with our previous observations.[13]

3.2. "Conventional" Substrates: Teflon, Polycarbonate, and Silicon Wafer. To further elucidate the relationship between evaporation modes, wetting hysteresis, and surface roughness, experiments were conducted with the following three conventional substrates: (a) poly(tetrafluoroethylene) (Teflon), (b) silicon wafer, and (c) polycarbonate. Similar polymeric surfaces have been used in previous wetting and evaporation studies.[6−9] Our evaporation studies revealed a trend similar to that of the mixed SAMs on gold (Figure 4), although the initial contact angles increased (from silicon wafer to polycarbonate to Teflon) as the hydrophobicity of the substrate increased. The constant contact area mode (pinning) was first observed, and thereafter a switch to the constant contact angle mode (shrinking) occurred. Although the mode-switching trend was similar, distinct differences in the evaporation hysteresis, $\Delta\theta_{evap}$, were observed. As shown in Table 1, polycarbonate and silicon substrates exhibited much smaller $\Delta\theta_{evap}$ values than Teflon. More importantly, direct measurements of wetting hysteresis compared very well to $\Delta\theta_{evap}$, with the Teflon substrate showing the largest value. The results for these three systems generalize our finding that the evaporation mode switching correlates with the wetting hysteresis of the surface and that evaporation plots can be used to evaluate the wetting hysteresis.

Yet, clear differences among these three substrates are noticeable. On relatively smooth surfaces, such as polycarbonate and silicon, the energy barrier impeding the movement of the solid−liquid−vapor three-phase contact line is small; therefore, the constant contact area mode does not dominate the course of evaporation.[24] In this case, the switch to the constant contact angle mode occurs more readily, that is, during the first 5 min of evaporation (Figure 4). In contrast, on Teflon the constant contact area mode persists for a fairly long period of time (more than 10 min). This is due to a rougher surface pinning the contact line of a drop to a greater extent,[27] that is, the drop sticks more tightly to the surface and must overcome a larger energy barrier to decrease its area.[24]

The correlation between the mode-switching trend, specifically, the contact angle hysteresis (from both evaporation and

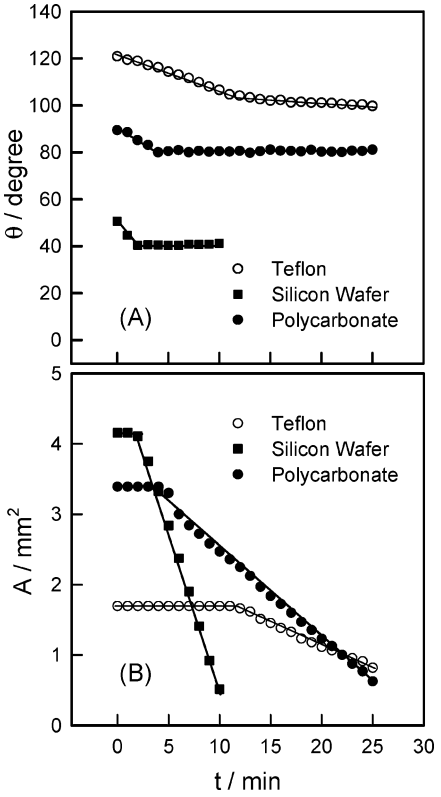

Figure 4. Evaporation of water microdroplets from conventional substrates (Teflon, silicon, and polycarbonate) under ambient conditions. (A) Contact angle as a function of evaporation time. (B) Contact area as a function of time.

direct measurements) and the roughness of the substrates were further evaluated by AFM topography studies (Figure 5). It appears that within a certain range of roughness the hysteresis values are similar, for example, approximately 10° for both polycarbonate and silicon wafers (although their RMS roughness factors are slightly different). Because the latter were only cleaned in piranha solution without further treatments (for example, chemical etching in NH_4F), the surface had a thin silicon oxide layer that is not atomically flat.[28] Therefore, the silicon samples showed a contact angle hysteresis comparable to that of polycarbonate and mixed SAMs on gold.

For Teflon the RMS roughness factor is more than double those of the other two systems, and its wetting hysteresis is also considerably higher. These results agree with the previous finding that when the surface roughness increases, the contact angle hysteresis will increase accordingly. In addition, we believe that this high degree of roughness for this particular brand of Teflon substrates is responsible for the observed high initial contact angle (120°) in comparison to reported literature values of approximately 108° for similar materials.[29]

The evaporation rates were also found to decrease nonlinearly with time in all cases (Figure 6). Similar to the mixed SAMs, a linear relationship was derived by plotting $V^{2/3}$ versus t using the spherical drop assumption.[4,26] As the hydrophobicity of the surface increased (from silicon to polycarbonate to Teflon). the evaporation rate decreased, as indicated by the longer lifetime of the water microdroplets. The different time scales for the entire evaporation process presented in Figures 3 and 6 may be due to the variability of the hydrophilicity of each substrate (different drop volumes were necessary to obtain stable droplets of a fairly symmetrical shape) and the atmospheric conditions (relative humidity and room temperature) that were not precisely controlled. While this certainly deserves further investigations,

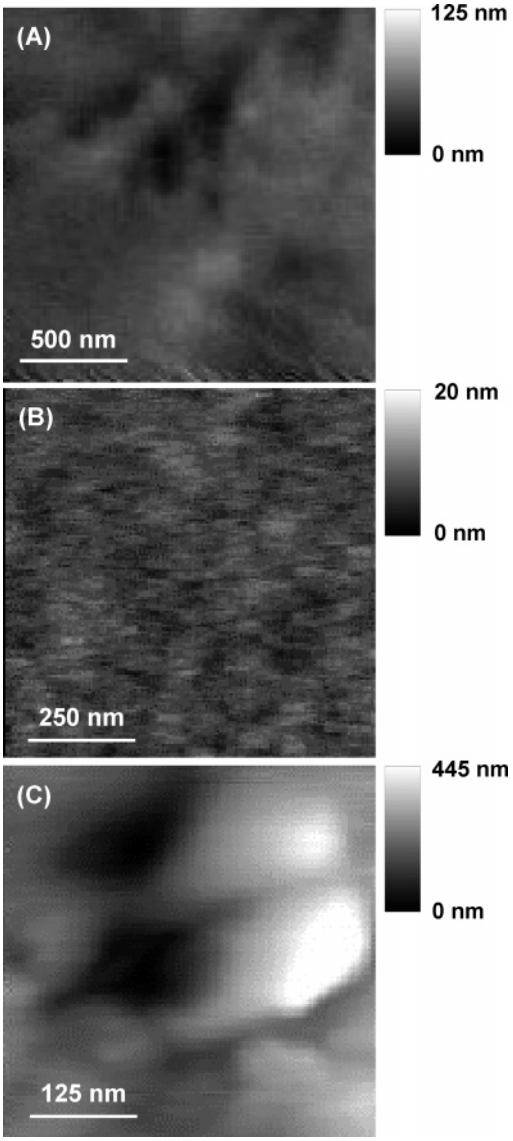

Figure 5. AFM images of conventional substrates: (A) polycarbonate base of CDs; (B) silicon wafers; and (C) Teflon sheets.

it is beyond the main focus (i.e., the evaporation modes and the correlation with wetting properties) of this study.

4. Discussion

The present study substantiates that the evaporation mode switching is a direct manifestation of wetting hysteresis, as was confirmed for not only model SAM surfaces but also for conventional substrates. In conducting direct measurements of wetting hysteresis using the method of Dettre and Johnson (where the advancing angle is found by increasing the drop volume until the contact area begins to advance, and the receding angle by decreasing the drop volume until the contact area begins to decrease),[20] we are essentially mimicking the process of evaporation where a droplet formed on a surface has an initial advancing front and, as evaporation proceeds, its volume decreases in constant contact area mode until the receding angle is attained. At this point, as evaporation causes the droplet volume to further decrease, the constant contact angle mode becomes dominant. This interpretation of evaporation, particularly its relation to surface roughness, is key to understanding the observations of other researchers who have noted results apparently different from ours. For example, Birdi and Vu

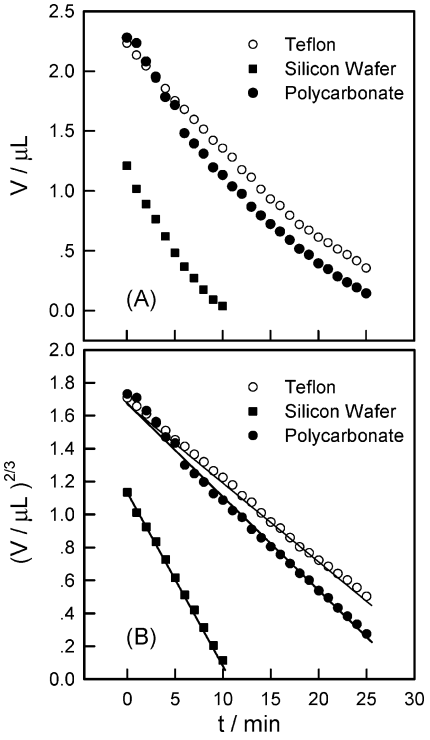

Figure 6. Evaporation rate of water microdroplets from conventional substrates. (A) Volume (V) as a function of evaporation time (t). (B) Linear relationship between $V^{2/3}$ and t.

observed only one mode for their substrates (glass and Teflon).[7] Their results may be explained by examining the very different surface topography of the two surfaces. For fairly rough surfaces, the contact line is pinned for a longer period, and the droplet may appear to evaporate in the constant contact area mode (decreasing angle). In this case, it is suggested that the receding contact angle θ_R has a value that is much smaller than the initial contact angle ($\theta_R << \theta_i$), therefore, a large hysteresis exists. Consequently, the switch to the constant contact angle mode may occur near the end of the evaporation process; depending on the increments of time measurements, this mode may be overlooked. Similarly, for smoother surfaces there is not much energy impeding the contact line; thus. the constant contact area mode may be easily missed because it is present for only a very short period during the initial stage of the evaporation (perhaps less than one minute), and the constant contact angle mode would appear to dominate the entire process. In this case, the receding angle is suggested to be close to the initial contact angle ($\theta_R \approx \theta_i$) and, as a result, the wetting hysteresis is approximately zero. Additional studies are warranted to confirm this hypothesis (for example, testing mixed SAMs on ultrasmooth gold surfaces[16]), with the challenge arising from measuring the wetting hysteresis at the limits where only one evaporation mode is observed and very small time intervals between measurements are needed.

Both chemical heterogeneity and surface roughness must be pondered before making generalizations about the dominant evaporation mode; it cannot be solely on the basis of whether a surface is hydrophobic or hydrophilic. Although it is not easy to unambiguously distinguish between the effects of surface roughness and chemical heterogeneity, we have shown that roughness plays a dominant role in the evaporation process on mixed SAMs on gold. In our previous study, the chemical heterogeneity of the surface was changed by varying the OH component of the SAMs; the effects due to surface roughness were insignificant as similar alkyl chain lengths of polar (C11OH) and nonpolar components (C10) were used.[13] We have found that varying the −OH content between 10 and 90% had no effect on the wetting hysteresis; a contact angle difference of approximately 10° always resulted, independent of the surface's hydrophobicity. This agrees with the results of Bain et al.[14] who directly measured the hysteresis on mixed SAMs (C11/C11OH), and with the earlier work of Holmes-Farley et al.[15] in which mixed monolayers formed from $HS(CH_2)_{15}COOH$ and $HS(CH_2)_{15}CH_3$ were tested with pH 3 water (to prevent ionization of the carboxy groups). Using ultrasmooth gold surfaces, Gupta et al.[16] also demonstrated recently that surface chemical heterogeneity does not contribute to contact-angle hysteresis in mixed SAMs. It should be noted that the similar wetting hysteresis (10°) on the C10/C11OH monolayers corresponds to the inclusive mode switching from the initial constant contact area to the subsequent constant contact angle mode.[13] Now we have shown that variations in roughness, even at the molecular scale, result in changes in the wetting hysteresis and, therefore, the timing for the evaporation mode switching.

Nevertheless, we note that this study is still limited in its ability to make a broad generalization of the evaporation phenomenon, as water was the only liquid studied and the experiments were carried out only under ambient conditions. Extended investigations are currently underway to evaluate the evaporation process with other solvents and surfaces in controlled environments.

5. Conclusions

In examining the evaporation of water microdroplets from model SAM surfaces and conventional substrates (Teflon, polycarbonate, and silicon), an inclusive mode switching behavior was observed. All surfaces exhibited an initial constant contact *area* mode and a subsequent constant contact *angle* mode. However, each surface showed a distinct evaporation hysteresis, $\Delta\theta_{evap}$ (taken as the difference between the initial contact angle and the averaged angle in the constant contact angle regime). Furthermore, $\Delta\theta_{evap}$ was found to be consistent with the directly measured wetting hysteresis ($\Delta\theta = \theta_A - \theta_R$). This demonstrates that evaporation plots can be solely used as a simple and reliable means to evaluate the wetting hysteresis. Analysis of the evaporation rates for each system revealed that the volumes decreased nonlinearly; however, plots of $V^{2/3}$ versus t showed a linear relationship. Generally, the more hydrophilic a surface, the faster is the evaporation rate. This study demonstrates that evaporation modes and rates are sensitive to changes in surface morphology on a scale as fine as the molecular level. It also shows that the data reported depend sensitively on the exact experimental conditions, thus rendering direct comparisons with literature observations difficult.

Acknowledgment. We thank the Natural Science and Engineering Research Council of Canada (NSERC) for financial support, and Dr. Eberhard Kiehlmann for reviewing the manuscript. D.M.S. acknowledges Dawn C. Armstrong, David Cross, Hidehiko Asanuma, and Marcus Kuikka for their help with some of the experiments.

References and Notes

(1) Rusdi, M.; Moroi, Y. *J. Colloid Interface Sci*. **2004**, *272*, 472−479.

(2) Hedestrand, G. *J. Phys. Chem.* **1924**, *28*, 1245−1252.

(3) Lurie, M.; Michailoff, N. *Ind. Eng. Chem.* **1936**, *28*, 345−349.

(4) Rowan, S. M.; Newton, M. I.; McHale, G. *J. Phys. Chem.* **1995**, *99*, 13268−13271.

(5) Erbil, H. Y.; McHale, G.; Newton, M. I. *Langmuir* **2002**, *18*, 2636−2641.
(6) Picknett, R. G.; Bexon, R. *J. Colloid Interface Sci.* **1977**, *61*, 336−350.
(7) (a) Birdi, K. S.; Vu, D. T. *J. Adhes. Sci. Technol*. **1993**, *7*, 485−493. (b) Birdi, K. S.; Vu, D. T. *J. Phys. Chem*. **1989**, *93*, 3702−3703.
(8) Bourgès-Monnier, C.; Shanahan, M. E. R. *Langmuir* **1995**, *11*, 2820−2829.
(9) Extrand, C. W. *Langmuir* **2004**, *20*, 4017−4021.
(10) Li, D.; Neumann, A. W. Wetting. In *Characterization of Organic Thin Films*; Ulman, A., Ed.; Butterworth-Heinemann: Woburn, MA, 1995; pp 165−192.
(11) Marmur, A. *J. Colloid Interface Sci.* **1994**, *168*, 40−46.
(12) For examples, see (a) Ulman, A. *Introduction to Ultrathin Organic Films, from Langmuir−Blodgett to Self-assembly*; Academic Press: New York, 1991. (b) Ulman, A. *Chem. Rev.* **1996**, *96*, 1533−1554.
(13) Yu, H. Z.; Soolaman, D. M.; Rowe, A. W.; Banks, J. T. *ChemPhysChem* **2004**, *5*, 1035−1038.
(14) Bain, C. D.; Evall, J.; Whitesides, G. M. *J. Am. Chem. Soc*. **1989**, *111*, 7155−7164.
(15) Holmes-Farley, S. R.; Bain, C. D.; Whitesides, G. M. *Langmuir* **1988**, *4*, 921−937.
(16) Gupta, P.; Ulman, A.; Fanfan, S.; Korniakov, A.; Loos, K. *J. Am. Chem. Soc.* **2005**, *127*, 4−5.
(17) Semal, S.; Bauthier, C.; Voué, M.; Vanden Eynde, J. J.; Gouttebaron, R.; De Coninck, J. *J. Phys. Chem. B* **2000**, *104*, 6225−6232.
(18) Folkers, J. P.; Laibinis, P. E.; Whitesides, G. M. *Langmuir* **1992**, *8*, 1330−1341.
(19) Evans, S. D.; Sharma, R.; Ulman, A. *Langmuir* **1991**, *7*, 156−161.
(20) Dettre, R. H.; Johnson, R. E. *J. Phys. Chem*. **1965**, *69*, 1507−1515.
(21) *Software Reference Manual*, Version. 5.01; Thermomicroscopes SPM Lab, California, 2000.
(22) It should be noted that the composition of a mixed monolayer does not necessarily reflect the composition of the deposition solution, as there is a preference for the adsorption of the longer alkanethiols as demonstrated by Folkers et al. (ref 18). We have also shown that in C10/C11OH SAMs formed from binary solutions there is preferential adsorption of the C10 component over the C11OH component (see Supporting Information, ref 13.). However, this does not detract from either the conclusion or the focus of the present study.
(23) Atre, S. V.; Liedberg, B.; Allara, D. L. *Langmuir* **1995**, *11*, 3882−3893.
(24) Yoshimitsu, Z.; Nakajima, A.; Watanabe, T.; Hashimoto, K. *Langmuir* **2002**, *18*, 5818−5822.
(25) Johnson, R. E.; Dettre, R. H. *Adv. Chem. Ser*. **1963**, *43*, 112−135.
(26) Erbil, H. Y.; Meric, R. A. *J. Phys. Chem. B* **1997**, *101*, 6867−6873.
(27) Gleiche, M.; Chi, L.; Gedig, E.; Fuchs, H. *ChemPhysChem* **2001**, *2*, 187−191.
(28) Fu, J.; Zhou, H.; Kramar, J.; Silver, R.; Gonda, S. *Appl. Phys. Lett*. **2003**, *82*, 3014−3015, and references therein.
(29) Chessick, J. H.; Healey, F. H.; Zettlemoyer, A. C. *J. Phys. Chem*. **1956**, *60*, 1345−1347.